

New catalytically active neodymium sulfate

Caridad Ruiz-Valero,* Concepción Cascales, Berta Gómez-Lor, Enrique Gutiérrez-Puebla, Marta Iglesias, M. Angeles Monge and Natalia Snejko

Instituto de Ciencia de Materiales de Madrid, CSIC, Campus de Cantoblanco, E-28049 Madrid, Spain. E-mail: crvalero@icmm.csic.es; Fax: 34 91372 0623; Tel: 34 91334 9026

Received 29th May 2002, Accepted 1st August 2002

First published as an Advance Article on the web 5th September 2002

Two novel isotopic rare earth sulfates, $R(\text{SO}_4)_2 \cdot \text{NH}_4$ ($R = \text{Nd}, \text{Eu}$), have been synthesized hydrothermally at 170 °C for 5 days. The crystal structures of these compounds have been established by single crystal X-ray diffraction to be the monoclinic space group $P2_1/c$, with $a = 8.867(1)$, $b = 7.187(1)$, $c = 10.804(2)$ Å, $\beta = 91.653(3)^\circ$ and $Z = 4$ for $\text{Nd}(\text{SO}_4)_2 \cdot \text{NH}_4$. The structure can be conceived as being formed of parallel layers $[\text{R}(\text{SO}_4)_2]^-$, in which a honeycomb (6, 3) layer of sharing edge RO_9 polyhedra is bonded to different isolated SO_4 tetrahedra. Inside the inter-block space a row of NH_4^+ ions are hosted, which connect the layers through hydrogen bonds. The magnetic measurements, and catalytic studies of the $\text{Nd}(\text{SO}_4)_2 \cdot \text{NH}_4$ in alkene hydrogenation, and selective oxidation of organic sulfides are reported. This material shows good activity and selectivity, and can be reused for at least four cycles without significant loss in catalytic activity.

Introduction

As a part of a systematic search for novel framework inorganic catalysts we have prepared $\text{R}(\text{SO}_4)_2 \cdot \text{NH}_4$ ($R = \text{Nd}, \text{Eu}$). Properties of rare earth sulfates and their derivatives have been poorly investigated. In fact, only studies on the synthesis and crystal structure determination have been carried out on these kinds of compounds.¹ Our interest² in these compounds have focussed on the study of the relationship between structure and their potential applications, mainly as catalysts, but also there is scope to study their magnetic and optical properties. To our knowledge the catalytic properties of rare-earth sulfates have scarcely been investigated.³ The catalytic hydrogenation of organic functional groups is probably the most common application of heterogeneous catalysis in the synthesis of organic compounds.⁴ The selective and rapid reduction of nitro compounds is of continued interest in view of the extensive synthetic application of this process. Homogeneous and heterogeneous catalysts have been extensively explored for use in this reaction. In the same way, catalytic oxidation is widely used in the manufacture of bulk chemicals from hydrocarbons and, more recently, as an attractive environmental method for the production of fine chemicals.^{5,6}

Here we report the syntheses and crystal structures of the two isomorphous Nd and Eu complexes, and some interesting catalytic properties together with the thermal and magnetic behavior of the Nd sulfate.

Experimental

General information

All reagents were commercially available and used as received. The IR spectrum was recorded from KBr pellets in the range 4000–320 cm^{-1} on a Perkin-Elmer spectrometer. Gas chromatography analysis (GC-MS) was performed using a Hewlett-Packard 5890 II with a flame ionization detector in a cross-linked methylsilicone column (a mixture of methylsilicone (OV-1701) and permethylcyclodextrin as the stationary phase).⁷ Thermogravimetric and differential thermal analysis (TGA-DTA) was performed on a SEIKO TG/DTA 320 apparatus in an atmosphere of air in the temperature range between 25 and 700 °C.

Synthesis

The compounds, $\text{R}(\text{SO}_4)_2 \cdot \text{NH}_4$ ($R = \text{Nd}, \text{Eu}$), were synthesized hydrothermally from a reaction of $\text{R}(\text{NO}_3)_3$ ($R = \text{Nd}, \text{Eu}$) (1 mmol), PrNH_2 (1 mL), and DMSO (14 mL). The mixture was heated in a 43 mL stainless steel reactor with a Teflon liner at 170 °C for 14 days.

The colourless crystals obtained were filtered and washed thoroughly with deionized water and ethanol. The Nd compound was obtained as the sole product of the reaction. The purity of the resulting microcrystalline powder product was checked by comparison between the experimentally observed and the calculated X-ray powder diffraction patterns.

Single crystal X-ray diffraction

Single crystals were resin epoxy coated and mounted on a Bruker SMART CCD diffractometer equipped with a normal focus, 2.4 kW sealed tube X-ray source (Mo- K_α radiation, $\lambda = 0.71073$ Å) operating at 50 kV and 40 mA. Data were collected over a hemisphere of reciprocal space by a combination of three sets of exposures. Each set had a different ϕ angle for the crystal and each exposure of 20 s covered 0.3° in ω . Unit cell dimensions were determined by a least-squares fit of 40 reflections with $I > 20\sigma(I)$. The first 30 frames of data were recollected at the end of the data collection to monitor crystal decay. The structure was solved by the Patterson method and refined in the monoclinic space group $P2_1/c$. After resolving the structure we found that these compounds were isotopic with $\text{KNd}(\text{SO}_4)_2$.⁸ Refinement was by full-matrix least-squares analysis with anisotropic thermal parameters for all non-hydrogen atoms and isotropic thermal parameters for the hydrogen atoms located in difference Fourier maps, but with bond lengths and angles restrained to idealized values.

All calculations were performed using SMART software for data collection, SAINT⁹ for data reduction, SHELXTL¹⁰ to resolve and refine the structure and to prepare material for publication, and ATOMS¹¹ for molecular graphics.

CCDC reference numbers 186877 and 186878.

See <http://www.rsc.org/suppdata/jm/b2/b205215f/> for crystallographic data in CIF or other electronic format.

X-Ray powder diffraction

The X-ray powder diffraction pattern for the Nd compound was taken at room temperature by using a Siemens D-500 diffractometer in the step scan mode with Cu-K α ($\lambda = 1.540598 \text{ \AA}$) radiation at a step value of 0.02° , measuring for 20 s at each step.

Magnetic measurements

Direct current magnetic measurements were carried out using a SQUID (Quantum Design) magnetometer operating from 2 to 400 K at 5000 Oe.

Catalytic reactions

Hydrogenation. The catalytic properties, in hydrogenation reactions of olefins (hex-1-ene, cyclohexene, 1-methylcyclohexene) and nitroaromatics (nitrobenzene, 2-nitrophenol, 2-nitrofluorene and 2-methyl-1-nitronaphthalene), of Nd(SO $_4$) $_2$ ·NH $_4$, were examined under conventional conditions for batch reactions in a reactor (Autoclave Engineers) of 100 mL capacity at 313 K, 4 atm. dihydrogen pressure and a metal : substrate molar ratio of 1 : 1000 for simple olefins and 1 : 100

Table 1 Hydrogenation of alkenes catalysed by Nd(SO $_4$) $_2$ ·NH $_4$

Substrate	Conv. (%) (t/min)	TOF ^a /mmol substrate (mmol cat. min ⁻¹)
Hex-1-ene	100(60)	2900
Cyclohexene	95(120)	1245
1-Methylcyclohexene	50(120)	700
Nitrobenzene	100(30)	1000
Nitrophenol	75(45)	350
2-Nitrofluorene	60(45)	140
2-Methyl-1-nitronaphthalene	55(45)	144

^aTurnover frequency.

Table 2 Crystal data and structure refinement for R(SO $_4$) $_2$ ·NH $_4$ (R = Nd, Eu)

	Nd(SO $_4$) $_2$ ·NH $_4$	Eu(SO $_4$) $_2$ ·NH $_4$
Formula	Nd(SO $_4$) $_2$ ·NH $_4$	Eu(SO $_4$) $_2$ ·NH $_4$
Formula weight/g mol ⁻¹	354.4	362.12
Crystal system	Monoclinic	Monoclinic
Space group	$P2_1/c$	$P2_1/c$
$a/\text{\AA}$	8.867 (1)	8.8605 (8)
$b/\text{\AA}$	7.187 (1)	7.1183 (7)
$c/\text{\AA}$	10.804 (2)	10.669 (1)
$\beta/^\circ$	91.653 (3)	91.324 (2)
Z	4	4
$V/\text{\AA}^3$	688.2 (2)	672.7 (1)
$\rho_{\text{calc}}/\text{Mg m}^{-3}$	3.42	3.575
μ/mm^{-1}	8.164	9.957
Dimensions	0.08 × 0.1 × 0.1	0.02 × 0.06 × 0.1
$F(000)$	668	680
Radiation	Mo K α ($\lambda = 0.71073 \text{ \AA}$)	Mo-K α ($\lambda = 0.71073 \text{ \AA}$)
Temperature/K	296 (2)	296 (2)
Diffractometer	Siemens Smart-CCD	Siemens Smart-CCD
Limiting indices (h,k,l)	(-2, -8, -12) to (10, 6, 13)	(-7, -10, -13) to (12, 3, 15)
θ range for data collected	3.40–26.58 $^\circ$	3.44–31.94 $^\circ$
Reflections collected	1819	3066
Independent reflections	1064	1590
R_{int}	0.083	0.044
Absorption correction	Sadabs	Sadabs
Max. and min. transmission	0.035 and 0.008	1.0 and 0.65
Refinement method	Full-matrix least-squares on F^2	Full-matrix least-squares on F^2
Goodness-of-fit on F^2	0.964	1.067
Final R indices [$I > 2\sigma(I)$]	$R1 = 0.066$, $wR2 = 0.154$	$R1 = 0.038$, $wR2 = 0.082$
R indices (all data)	$R1 = 0.086$, $wR2 = 0.162$	$R1 = 0.053$, $wR2 = 0.088$

Table 3 Selected bond lengths (\AA) and angles ($^\circ$) for R(SO $_4$) $_2$ ·NH $_4$ (R = Nd, Eu)

Distances	Nd	Eu
R(1)–O(2)	2.50 (1)	2.458 (5)
R(1)–O(3)	2.50 (1)	2.474 (5)
R(1)–O(3 ¹)	2.49 (1)	2.432 (5)
R(1)–O(4 ²)	2.44 (1)	2.405 (6)
R(1)–O(5 ³)	2.41 (2)	2.371 (6)
R(1)–O(6)	2.64 (1)	2.580 (5)
R(1)–O(6 ⁴)	2.50 (1)	2.493 (4)
R(1)–O(7)	2.51 (1)	2.461 (4)
R(1)–O(7 ⁵)	2.52 (2)	2.493 (5)
Angles		
O(2)–R(1)–O(3)	54.8 (4)	56.2 (2)
O(2)–R(1)–O(3 ¹)	119.7 (4)	120.2 (2)
O(2)–R(1)–O(4 ²)	78.5 (4)	78.5 (2)
O(2)–R(1)–O(5 ³)	95.5 (4)	95.0 (2)
O(2)–R(1)–O(6)	135.5 (4)	134.6 (2)
O(2)–R(1)–O(6 ⁴)	95.3 (4)	96.2 (2)
O(2)–R(1)–O(7)	155.6 (4)	156.0 (2)
O(2)–R(1)–O(7 ⁵)	71.9 (4)	71.1 (2)
O(3)–R(1)–O(3 ¹)	65.0 (4)	64.0 (2)
O(3)–R(1)–O(4 ²)	122.4 (4)	122.8 (2)
O(3)–R(1)–O(5 ³)	74.6 (4)	75.5 (2)
O(3)–R(1)–O(6)	154.2 (4)	153.7 (2)
O(3)–R(1)–O(6 ⁴)	75.9 (4)	75.8 (2)
O(3)–R(1)–O(7)	128.9 (4)	127.6 (2)
O(3)–R(1)–O(7 ⁵)	114.2 (4)	115.4 (1)
O(3 ¹)–R(1)–O(4 ²)	141.2 (4)	141.5 (2)
O(3 ¹)–R(1)–O(5 ³)	68.3 (5)	68.9 (2)
O(3 ¹)–R(1)–O(6)	99.9 (4)	99.8 (2)
O(3 ¹)–R(1)–O(6 ⁴)	67.6 (4)	68.5 (2)
O(3 ¹)–R(1)–O(7)	69.5 (4)	69.4 (2)
O(3 ¹)–R(1)–O(7 ⁵)	142.4 (4)	142.5 (2)
O(4 ²)–R(1)–O(5 ³)	148.6 (5)	147.6 (2)
O(4 ²)–R(1)–O(6)	82.8 (4)	83.0 (2)
O(4 ²)–R(1)–O(6 ⁴)	77.3 (4)	76.6 (2)
O(4 ²)–R(1)–O(7)	81.7 (4)	81.9 (2)
O(4 ²)–R(1)–O(7 ⁵)	73.5 (4)	73.1 (2)
O(5 ³)–R(1)–O(6)	80.4 (4)	79.3 (2)
O(5 ³)–R(1)–O(6 ⁴)	134.1 (4)	135.8 (2)
O(5 ³)–R(1)–O(7)	108.8 (4)	108.9 (2)
O(5 ³)–R(1)–O(7 ⁵)	75.3 (4)	74.8 (2)
O(6)–R(1)–O(6 ⁴)	119.3 (3)	119.3 (1)
O(6)–R(1)–O(7)	54.4 (4)	55.09 (1)
O(6)–R(1)–O(7 ⁵)	64.2 (4)	63.9 (2)
O(6 ⁴)–R(1)–O(7)	66.2 (4)	65.7 (2)
O(6 ⁴)–R(1)–O(7 ⁵)	149.9 (4)	148.9 (2)
O(7)–R(1)–O(7 ⁵)	115.8 (3)	116.0 (1)

^aSymmetry transformations used to generate equivalent atoms: 1 = ($-x + 2, -y, -z + 1$); 2 = ($x, -y + \frac{1}{2}, z + \frac{1}{2}$); 3 = ($x, -y + \frac{1}{2}, z - \frac{1}{2}$); 4 = ($-x + 2, y - \frac{1}{2}, -z + \frac{3}{2}$); 5 = ($-x + 2, y + \frac{1}{2}, -z + \frac{3}{2}$).

for nitroaromatics. The results were monitored by GLC (gas liquid chromatography) using an internal standard reference. After hydrogenation, the catalyst was removed by filtration and used again. The kinetic results are shown in Table 1.

Oxidation of sulfides. The oxidation of methyl phenyl sulfide was carried out in a batch reactor at atmospheric pressure, 343 K, and using 1,2-dichloroethane as solvent (5 mL). 10 mg of the catalyst were stirred in a suspension containing the solvent and 1.0 mmol of the thioether. The oxidant (H $_2$ O $_2$, 30%, 3 eq.) was added dropwise, while the overall suspension was heated up to 343 K. Samples were taken at regular times and analyzed by GLC.

Results and discussion

Crystal structure

A summary of the fundamental crystal data for R(SO $_4$) $_2$ ·NH $_4$ (R = Nd, Eu) is given in Table 2, and selected bond distances and angles are given in Table 3.

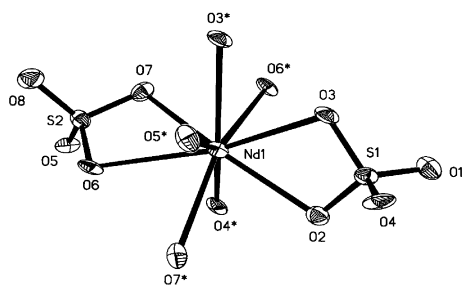


Fig. 1 Labeled ORTEP plot of the building block unit in $\text{Nd}(\text{SO}_4)_2 \cdot \text{NH}_4$; asterisks indicate atoms that are symmetrically related according to Table 3.

In these materials the R ions are surrounded by nine oxygen atoms, Fig. 1, with distances from 2.41(1) to 2.64(1) Å, and from 2.371(6) to 2.580(5) Å, for Nd and Eu respectively. The two independent sulfur atoms show the classical tetrahedral environment with distances and angles similar to those found^{1–7} in other sulfate compounds. The RO_9 polyhedra are sharing two edges in the *b*-direction, and one in the *c*-direction. The structure can be conceived as being formed by layers $[\text{R}(\text{SO}_4)_2]^-_\infty$ parallel to the *bc* plane, Fig. 2, in which a honeycomb (6, 3) layer of edge sharing RO_9 polyhedra is bonded to different isolated SO_4 tetrahedra. These layers are bent in the *a* direction, as can be seen in Fig. 3. Given that a longer S–O distance in the SO_4^{2-} anions is not observed, the possibility of there being a hydrogen sulfate is discarded. As a cation is needed to maintain the electrical neutrality, it seems quite plausible to think that the molecule per formula located in the interlayer space could be an ammonium cation. The hydrogen atoms in this cation were located and the distances from the nitrogen atom to the nearest oxygen atoms 2.875(5), 2.89(2), and 2.90(4) Å are typical of distances between NH_4^+ ions and surrounding oxygen atoms (Table 4). The IR spectrum of the Nd material exhibits two sharp peaks in the area 1405–1460 cm^{-1} corresponding to the NH_4^+ group vibrations. The characteristic bands of the sulfate groups appear in the usual regions of 970–990, ≈ 470 , 1025–1250, and 580–660 cm^{-1} for ν_1 – ν_4 , respectively, some of them being split into two or more bands. The absence of any strong absorption bands in the area 3000–3500 cm^{-1} confirms the absence of coordinated molecules of water in the structure.

The TGA-DTA analysis shows a weight loss between 420 and 480 °C, accompanied by an endothermic peak which

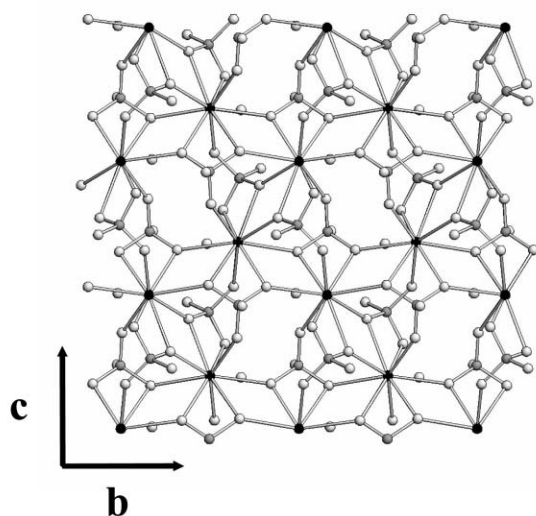


Fig. 2 View along the [100] direction of the structure of $\text{Nd}(\text{SO}_4)_2 \cdot \text{NH}_4$.

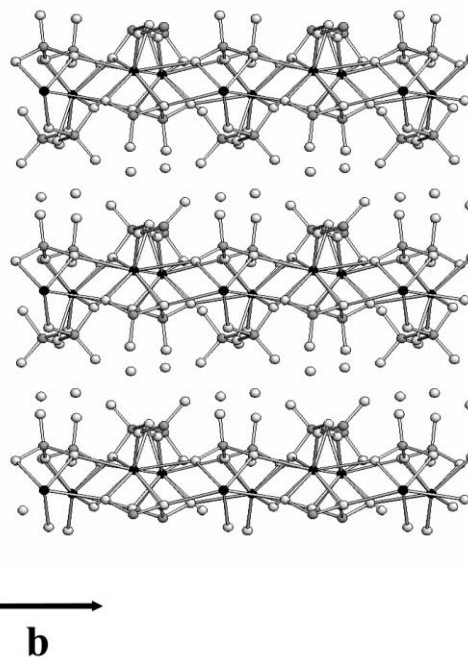


Fig. 3 View along the [001] direction, showing the ∞ layers $[\text{Nd}(\text{SO}_4)_2]$.

Table 4 N–H \cdots O hydrogen bond lengths (Å) and angles (°) for $\text{R}(\text{SO}_4)_2 \cdot \text{NH}_4$ (R = Nd, Eu)

	Nd	Eu		Nd	Eu
N1–H11	0.93 (8)	0.93 (6)	N1–O1	2.89 (2)	2.875 (5)
N1–H12	0.93 (8)	0.93 (6)	N1–O2	2.90 (1)	2.904 (6)
N1–H13	0.92 (8)	0.93 (6)	N1–O4	3.06 (1)	3.053 (5)
N1–H14	0.92 (8)	0.93 (6)	N1–O8	2.97 (1)	2.958 (5)
H11 \cdots O1	2.32 (8)	2.13 (6)	N1–H11 \cdots O1	120 (2)	136 (1)
H11 \cdots O8	2.28 (8)	2.35 (6)	N1–H11 \cdots O8	143 (2)	129 (1)
H12 \cdots O8	2.07 (8)	2.07 (6)	N1–H12 \cdots O8	174 (2)	148 (1)
H13 \cdots O1	2.27 (8)	2.22 (6)	N1–H13 \cdots O1	124 (2)	86 (1)
H13 \cdots O2	2.43 (8)	2.18 (6)	N1–H13 \cdots O2	111 (2)	134 (1)
H14 \cdots O4	2.37 (8)	2.15 (6)	N1–H14 \cdots O4	132 (2)	163 (1)

corresponds to the transformation of $\text{Nd}(\text{SO}_4)_2 \cdot \text{NH}_4$ to the monoclinic $\text{Nd}_2(\text{SO}_4)_3$ (PDF 83-2244), this latter phase remains unchanged up to 700 °C. The decomposition temperature for this compound matches exactly the decomposition temperatures for $\text{M}(\text{SO}_4)_2 \cdot \text{NH}_4$ type compounds.¹²

Due to the following features of this structure, i) edge sharing NdO_9 polyhedra containing layers, ii) unhindered access and coordination of the substrate molecules during the intermediate steps of catalytic reactions, and iii) thermal stability up to 400 °C, it seemed quite interesting to check the existence of magnetic order in the Nd^{3+} cations, as well as, the catalytic activity of this new sulfate.

Magnetic properties

The temperature dependence of the molar d.c. magnetic susceptibility χ , and its reciprocal, is shown in Fig. 4 for the Nd compound. Above ~ 90 K the plot follows a Curie–Weiss type behavior, $\chi^{-1} = [35.5(2) + 0.7875(8)T]$ mol emu^{-1} ($r = 0.99991$). The calculated magnetic moment is 3.2 μ_B , which agrees well with the expected value, 3.6 μ_B , for the free-ion ground term $^4I_{9/2}$ of the Nd^{3+} ion. Since no maxima in χ are observed at low temperatures, it is clear that under 90 K the effect of the crystal-field splitting of this ground term is responsible for the downward deviation from linearity in the χ^{-1} vs. T plot. Therefore, the Weiss constant for the material, $\theta_c = -45$ K, is entirely due to crystal-field effects.

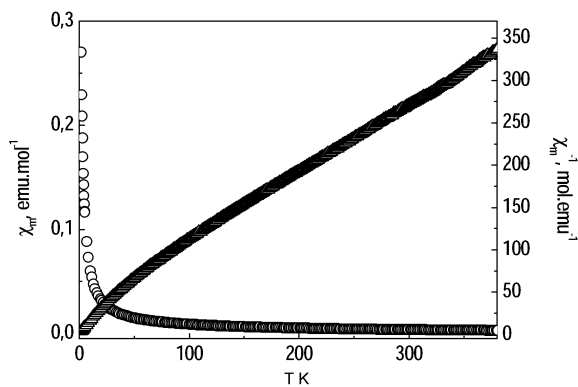


Fig. 4 Magnetic susceptibility χ , and its reciprocal, plotted as a function of temperature, for $\text{Nd}(\text{SO}_4)_2 \cdot \text{NH}_4$.

Catalytic properties

The performance of $\text{Nd}(\text{SO}_4)_2 \cdot \text{NH}_4$ as a hydrogenation catalyst was tested in reactions with olefins (hex-1-ene, cyclohexene, and 1-methylcyclohexene), Fig. 5a, and nitroaromatics (nitrobenzene, 2-nitrophenol, 2-nitrofluorene and 2-methyl-1-nitronaphthalene), Fig. 5b. Quantitative yields were obtained for all substrates studied over 1–3 h. As can be seen, alkenes were hydrogenated without an induction period, and isomerization was not detected, Fig. 5. The maximum rate of hydrogenation of the three olefins decreased in the order hex-1-ene > cyclohexene > 1-methylcyclohexene. It seems that the enhanced surface concentration effect and/or an electrical interaction between the substrate and the material could indeed be responsible for the absence of an induction period. The turnover frequency is reported in Table 1. The

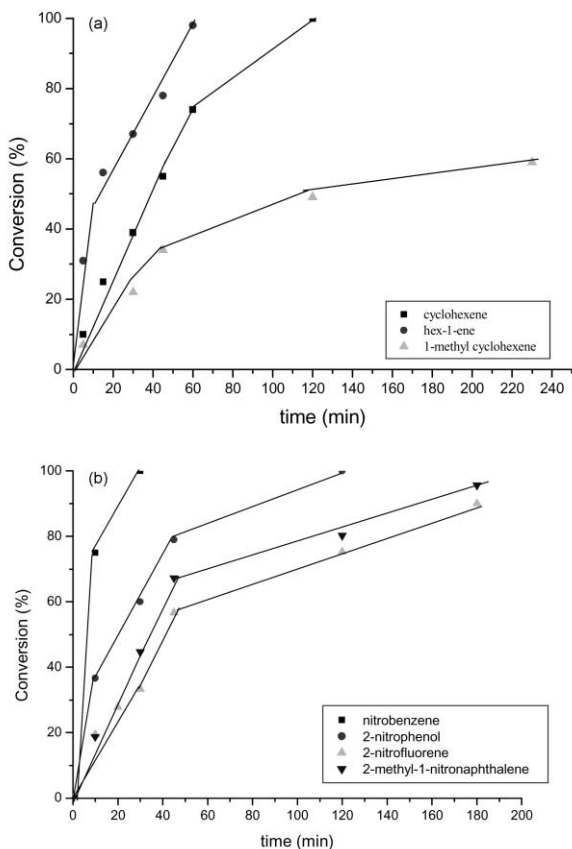


Fig. 5 Kinetic profile (a) for the hydrogenation of alkenes (b) for the reduction of nitroaromatics catalysed by $\text{Nd}(\text{SO}_4)_2 \cdot \text{NH}_4$.

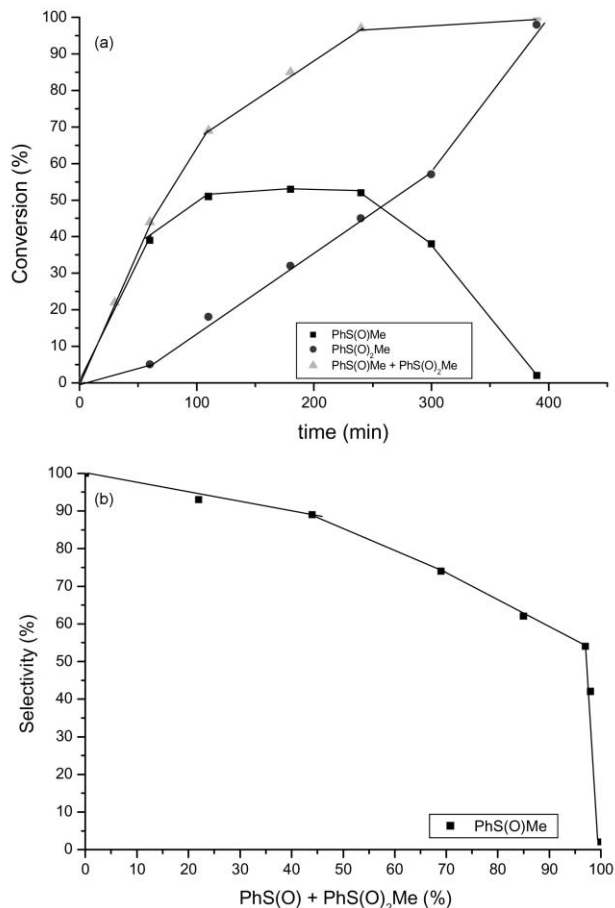


Fig. 6 (a) Kinetic profile and (b) selectivity curve for the catalytic oxidation of methyl phenyl sulfide with $\text{Nd}(\text{SO}_4)_2 \cdot \text{NH}_4$.

reduction of nitroaromatics (Fig. 5b) proceeded with high yields and the turnover frequencies were in the range of $1000\text{--}145\text{ min}^{-1}$. The most important characteristic of our catalytic system is the reduction of the bulky molecules, 2-nitrofluorene and 2-methyl-1-nitronaphthalene, in 100% yield within 3 h. The catalyst was reused without any reactivation at least four times.

The oxidation of organic sulfides was usually carried out in the presence of catalytic amounts of catalyst (0.04% based on experimental metal content) by using hydrogen peroxide (H_2O_2) as the sacrificial oxidant in 1,2-dichloroethane at 343 K. The catalyst appeared to be stable under experimental conditions, since the catalyst recovered by filtration of the reaction mixture and washing with 1,2-dichloroethane was found to be reactive for further catalytic runs. The results are shown in Fig. 6. The kinetic profile shows a high initial reaction followed by a decrease in activity. The selectivity curve shows that the sulfoxide is a primary and unstable product, while the corresponding sulfone appears as a secondary and stable product.

In conclusion, we present the synthesis, structure, magnetic measurements and catalytic studies of the first rare earth sulfate used in olefin hydrogenation and sulfide oxidation. The advantages of our catalytic system compared to others are: i) it is simple, ii) the reaction conditions are mild, iii) reduction of the bulky molecules was carried out easily eliminating the use of expensive reagents, iv) reusability of the catalyst.

Acknowledgements

The authors thank the Spanish DGI of MCT MAT2001-1433, and CAM Ref. 07N/0003/2001 for support of this work.

References

- 1 M. S. Wickleder, *Z. Anorg. Allg. Chem.*, 1998, **624**(8), 1347–1354; G. Sherry, *J. Solid State Chem.*, 1976, **19**, 271; M. S. Wickleder, *Z. Anorg. Allg. Chem.*, 1999, **625**(9), 1548–1555; A. C. Blackburn and R. E. Gerkin, *Acta Crystallogr. Sect. C*, 1994, **50**, 835–838; P. C. Junk, C. J. Kepert, B. W. Skelton and A. H. White, *Austr. J. Chem.*, 1999, **52**(6), 601; M. S. Wickleder, *Z. Anorg. Allg. Chem.*, 1998, **624**(10), 1583–1587; M. S. Wickleder, *Chem. Mater.*, 1998, **10**, 3212–3216.
- 2 C. Cascales, E. Gutiérrez-Puebla, M. A. Monge and C. Ruiz-Valero, *Angew. Chem., Int. Ed.*, 1998, **37**(1), 129–131; C. Cascales, E. Gutiérrez-Puebla, M. A. Monge and C. Ruiz-Valero, *Int. J. Inorg. Mater.*, 1999, **1**, 181–186; C. Cascales, E. Gutiérrez-Puebla, M. A. Monge and C. Ruiz-Valero, *Angew. Chem., Int. Ed.*, 1999, **38**, 129; C. Cascales, E. Gutiérrez-Puebla, M. Iglesias, M. A. Monge, C. Ruiz-Valero and N. Snejko, *Chem. Commun.*, 2000, 2145–2146; B. Gomez-Lor, M. Iglesias, C. Cascales, E. Gutiérrez-Puebla and M. A. Monge, *Chem. Mater.*, 2001, **13**, 1364; B. Gomez-Lor, E. Gutiérrez-Puebla, M. Iglesias, M. A. Monge, C. Ruiz-Valero and N. Snejko, *Inorg. Chem.*, 2002, **41**, 2429–2432; N. Snejko, E. Gutiérrez-Puebla, J. L. Martínez, M. A. Monge and C. Ruiz-Valero, *Chem. Mater.*, 2002, **14**, 1879–1883; N. Snejko, C. Cascales, B. Gómez-Lor, E. Gutiérrez-Puebla, M. Iglesias, C. Ruiz-Valero and M. A. Monge, *Chem. Commun.*, 2002, 1366–1367; C. Cascales, B. Gomez-Lor, E. Gutiérrez Puebla, M. Iglesias, M. A. Monge, C. Ruiz-Valero and N. Snejko, *Chem. Mater.*, 2002, **14**, 677–681.
- 3 Z.-K. Lu and W.-R. Zu, *Chin. J. Org. Chem.*, 2000, **20**(5), 819–821.
- 4 R. L. Augustine, *Catal. Today*, 1997, **37**, 419–440.
- 5 R. A. Sheldon, *Chemtech*, 1991, 556.
- 6 R. A. Sheldon, *J. Mol. Catal. A: Chem.*, 1996, **107**, 75.
- 7 E. Miranda, F. Sánchez, J. Sanz, M. I. Jiménez and I. Martínez-Castro, *J. High Resol. Chromatogr.*, 1998, **21**, 225.
- 8 L. D. Iskhakova, Y. Gasanov and V. K. Trunov, *Zh. Strukt. Khim.*, 1988, **29**, 95–99.
- 9 Siemens, *SAINTE. Data Collection and Procedure. Software for the SMART System*, Siemens Analytical X-ray Instruments Inc., 1995.
- 10 SHELXTL, Siemens Energy & Automation Inc., Analytical Instrumentation, Madison, Wisconsin, USA, 1996.
- 11 E. Dowty, *ATOMS for Windows 3.1. A Computer Program for Displaying Atomic Structure*, 521 Hidden Valley Road. King-sport. TN37663, USA, 1995.
- 12 T. Erämetsä and L. Niinistö, *Suom. Kemistil. B*, 1971, **44**, 107.